Publication P2

Seman, S., Kanerva, S., Niiranen, J., Arkkio, A. 2004. "Transient Analysis of Wind Power Doubly Fed Induction Generator Using Coupled Field Circuit Model", *Proceedings of ICEM 2004*, 5-8 September 2004, Cracow, Poland, 6 p., (CD-ROM).

Transient Analysis of Doubly Fed Wind Power Induction Generator Using Coupled Field-Circuit Model

S. Seman*, S. Kanerva*, J. Niiranen, A. Arkkio***

* Laboratory of Electromechanics, Helsinki University of Technology P.O.Box 3000, 02015 HUT, Finland
e-mail slavomir.seman@hut.fi, sami.kanerva@hut.fi, antero.arkkio@hut.fi

** ABB Oy, P.O. Box 186, FIN-00381, Helsinki, Finland, e-mail jouko.niiranen@fi.abb.com

Abstract — **The paper presents the transient analysis of a 1.7 MVA wind-power doubly fed induction generator (DFIG) connected to the network and controlled by modified direct torque control during power system disturbances. The finite element model of DFIG is coupled with circuit models of frequency converter, transformer, network and control part in Matlab-Simulink. The transient currents and electromagnetic torque obtained from DFIG finite element model are compared with the simulation results obtained by means of an equivalent circuit-based analytical model with constant lumped parameters.**

I. INTRODUCTION

The wind-power doubly fed induction generators are nowadays more widely used especially in large wind farms. The main reason for the increase of number of wind turbines with DFIG connected to the national networks is mainly their ability to supply power at constant voltage and frequency while the rotor speed varies. DFIG wind turbine utilizes a wound rotor induction machine while the rotor winding is supplied from rotor-side frequency converter providing speed control together with terminal voltage and power factor control for the overall system.

Due to the increase in the number of wind turbines connected to the network, the new network codes were issued prescribing how the wind generator has to support the network during the power disturbances in the network [1]. Therefore it is necessary to carry out accurate transient simulations in order to understand the impact of the power system disturbances on a wind turbine operation.

The most common approach in dynamic modeling of DFIG wind turbines is using an analytical equivalent circuit based model of the doubly fed induction machine [2]-[6]. However, simple analytical models of DFIG usually don't represent magnetic saturation of the leakage and magnetizing inductance accurately or not at all. The saturation needs to be taken into account when simulating the transients in rotor and stator currents in order to get more accurate results.

This paper presents the transient simulation analysis of a 1.7 MVA DFIG wind turbine under symmetrical network 3-phase short circuit The doubly fed induction generator is simulated by means of finite element method (FEM) whereas frequency converter, transformer, network and control part are modeled in Matlab-Simulink. The rotor-side frequency converter is controlled by a modified direct torque control (DTC) control strategy. The rotor over-current protection, so called passive crowbar [7], which protects the rotor of DFIG and rotor-side frequency converter during network disturbances when the generator supports the network, is also included in circuit simulator.

The transient stator current, rotor current and electromagnetic torque calculated by means of DFIG finite element method model are compared with simulation results obtained by means of an equivalent circuit based analytical model with constant lumped parameters.

II. FINITE ELEMENT MODEL OF DFIG

The FEM computation is based on two-dimensional vector potential formulation coupled with the voltage equations of the windings [9]. The magnetic vector potential A satisfies

$$-\nabla \cdot (\nu \nabla A) = J \tag{1}$$

where ν is the nonlinear reluctivity. The current density J is determined by

$$J = \frac{Ni}{S} \tag{2}$$

in a phase winding with cross section area S and N filaments carrying the current i, and

$$J = -\sigma \frac{\partial A}{\partial t} \tag{3}$$

in solid conductors with conductivity σ. Since there are no damping bars in the rotor, (3) only contains the effect of eddy currents in the steel shaft. In the laminated iron core, conductivity is set to zero for simplicity.

The voltage equations for the windings are in the form

$$u = \frac{\mathrm{d}\psi}{\mathrm{d}t} + Ri + L_{\mathrm{e}} \frac{\mathrm{d}i}{\mathrm{d}t} \tag{4}$$

where R is the total resistance of the coil and L_{e} is the additional end-winding inductance. The flux linkage ψ is determined by adding together the contributions of all coil sides in the winding

$$\psi = \sum_{k=1}^{n_{\mathrm{c}}} \beta_k A_k^{\mathrm{ave}} l_k \tag{5}$$

where n_{c} is the total number of coil sides in the winding, β_k is either positive or negative multiplier according to the orientation of the coil side k, A_k^{ave} is the average vector potential on the coil side and l_{k} is the length of the coil side k.

The sources of the field analysis are the voltages applied in the phase windings in stator and rotor. The magnetic vector potential and phase currents are obtained from the simultaneous solution of the above equations.

The electromagnetic torque T_e is determined from the field solution using the virtual work principle

$$T_e = \frac{d}{d\theta} \int_{\Omega} \int_0^H \boldsymbol{B} \cdot d\boldsymbol{H} \, d\Omega \tag{6}$$

where θ is the position angle of the rotor and Ω is the cross section of the air gap. The magnetic flux density $\boldsymbol{B}$ and the magnetic field strength $\boldsymbol{H}$ are determined from the field solution in terms of A and ν. The angular speed and position of the rotor are solved from

$$\omega_m = \int \frac{1}{J} \left(T_e - T_L \right) dt \tag{7}$$

$$\theta = \int \omega_m dt \tag{8}$$

where J is the moment of inertia and T_L is the load torque. The movement of the rotor is modeled by modifying the air-gap mesh.

The FEM computation is implemented as a functional block in Simulink using dynamically linked program code (S-function). Voltage of the phase windings in stator and rotor are given as input variables and the phase currents, electromagnetic torque, rotor position and flux linkage in stator and rotor are obtained as output variables. This is illustrated in Figure 1.

Before the simulation, the initial magnetic field in the electrical machine is calculated by time-harmonic steady-state analysis when sinusoidal voltages and currents are assumed [9]. The information about the magnetic field and finite element mesh is stored in a text file or Matlab's MAT-file, which is read by the S-function in the beginning of the simulation. After the time-stepping simulation, the magnetic field is stored in a new file that can be used as the initial condition for a new simulation.

In time-stepping simulation, the FEM computation is coupled with Simulink by weak coupling procedure. This means that the time-stepping FEM computation runs at major time steps, which are usually longer than the minor steps elsewhere in the system model in Simulink. Accordingly, output variables from FEM computation are kept constant during a period of several simulation steps in the total system model, and changes in the variables take effect with one-step delay. The procedure of the FEM calculation in major steps is characterized by Figure 2.

In spite of the weak coupling, the accuracy of the coupled solution can be maintained by choosing the time steps appropriately according to the physical time constants. By using short steps in the converter model and longer steps in the FEM model, the time-stepping simulation is also more efficient, because the time-consuming FEM solution is not determined too frequently.

The finite element mesh of the DFIG covers one quarter of the cross section, comprising 949 nodes and 1848 linear triangular elements. With quadratic elements, the number of nodes increases to 3745 and the computation time also increases remarkably. Nevertheless, the differences in the current and voltage waveforms are not very significant in comparison between linear and quadratic elements. The geometry of the model is presented in Figure 3, and the ratings of the DFIG are presented in Table I.

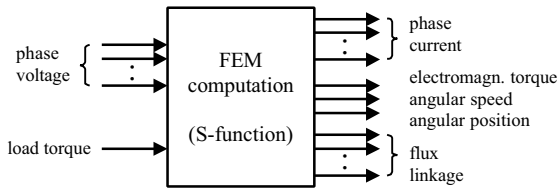

Figure. 1. Functional block of the FEM computation.

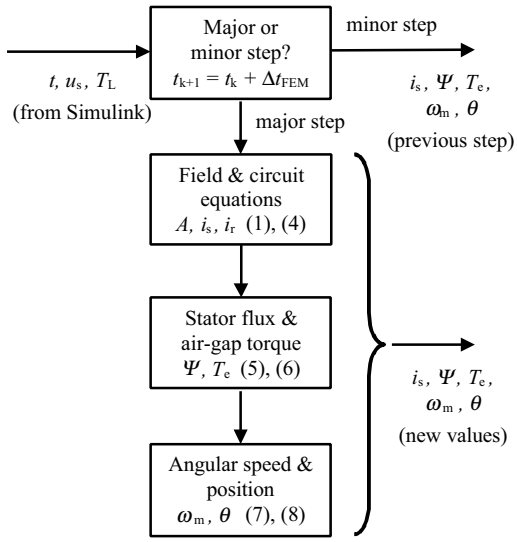

Figure 2. FEM calculation in time stepping analysis.

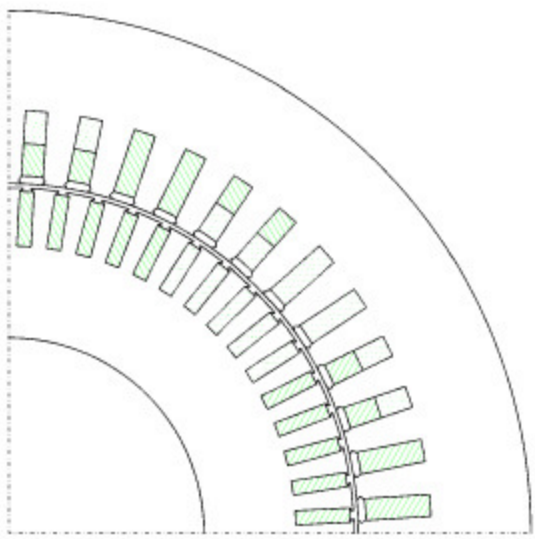

Figure 3. Geometry of the DFIG model.

TABLE I PARAMETERS OF THE DFIG

P_N	rated power	1.7 MW
$U_{N,s}$	rated stator voltage	690 V (delta)
$U_{max,r}$	maximum rotor voltage [1]	2472 (star)
f_N	rated stator frequency	50 Hz
n_N	nominal speed	1500 rpm

[1] In normal use rotor voltage is proportional to slip

III. FREQUENCY CONVERTER AND CONTROL

The Frequency converter that supplies the rotor of DFIG consists of two back-to-back connected voltage source inverters as it is depicted in Figure 4.

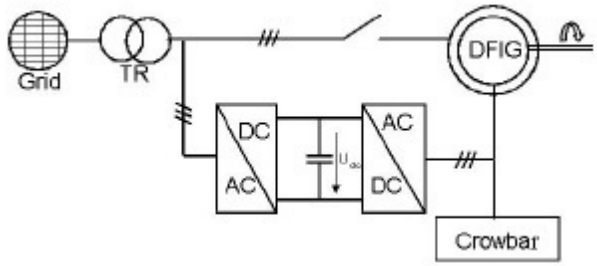

Figure 4. Doubly fed wind-power induction generator with the crowbar.

The network-side converter is represented in simulation by discrete transfer function

$$H(z) = \frac{1}{1+\tau_s z^{-1}} \tag{9}$$

where τ_s denotes the time constant of the first order discrete filter. The aim of the control of the network side inverter is to maintain the level of DC-link voltage U_{dc} on a pre-set value. U_{dc} is controled by PI controler based algorithm.

The control of the rotor side frequency converter is realized by a modified DTC strategy [8] as it is depicted in Figure 5.

The magnitude of the rotor flux estimate $|\hat{\psi}_r|$ is calculated by means of Torque and Flux estimator from the measured rotor currents i_{ra}, i_{rb}, as

$$|\hat{\psi}_r| = \sqrt{(\hat{\psi}_{r\_x})^2 + (\hat{\psi}_{r\_y})^2} \tag{10}$$

where symbols $\hat{\psi}_{r\_x}$ and $\hat{\psi}_{r\_y}$ denote the estimated rotor fluxes in the two axis reference frame fixed to the rotor.

The rotor flux estimates are

$$\hat{\psi}_{r\_x} = L_r i_{rx} + L_m i_{sx\_r} \tag{11}$$

$$\hat{\psi}_{r\_y} = L_r i_{ry} + L_m i_{sy\_r} \tag{12}$$

where i_{rx}, i_{ry} denote the rotor current components in the two-axis rotational reference frame and i_{sx_r}, i_{sy_r} denote the stator currents in the rotational frame.

The magnitude of the grid flux estimate $|\hat{\psi}_{grid}|$ that is used in control for synchronization of DFIG with network is also calculated in Torque and Flux estimator from the measured stator currents i_{sA}, i_{sB} and stator voltages v_{sA}, v_{sB}.

The estimate of electromagnetic torque that is an input of the three-level hysteresis comparator is given by

$$\hat{T}_e = \frac{3}{2} p \left(i_{y\_s}\hat{\psi}_{x\_s} - i_{x\_s}\hat{\psi}_{y\_s} \right) \tag{13}$$

Where symbols i_{x_s}, i_{y_s} and $\hat{\psi}_{x\_s}$, $\hat{\psi}_{y\_s}$ denote the stator currents and estimated stator fluxes respectively in two-axis stator frame.

The reference value of the rotational speed ω_r is considered to be constant. The reference value of rotor flux magnitude is obtained from the reference flux calculator as function of the power factor PF_ref and electromagnetic torque reference value T_{e_ref}.

The torque and flux hysteresis comparators provide logical output that is used together with estimated rotor fluxes for switching pattern establishment defined by an optimal switching table.

When the switching pattern is established, a voltage phasor is applied to the rotor and this voltage will change the rotor flux. The tangential component of the voltage vector controls the torque whereas the radial component increases or decreases the flux magnitude.

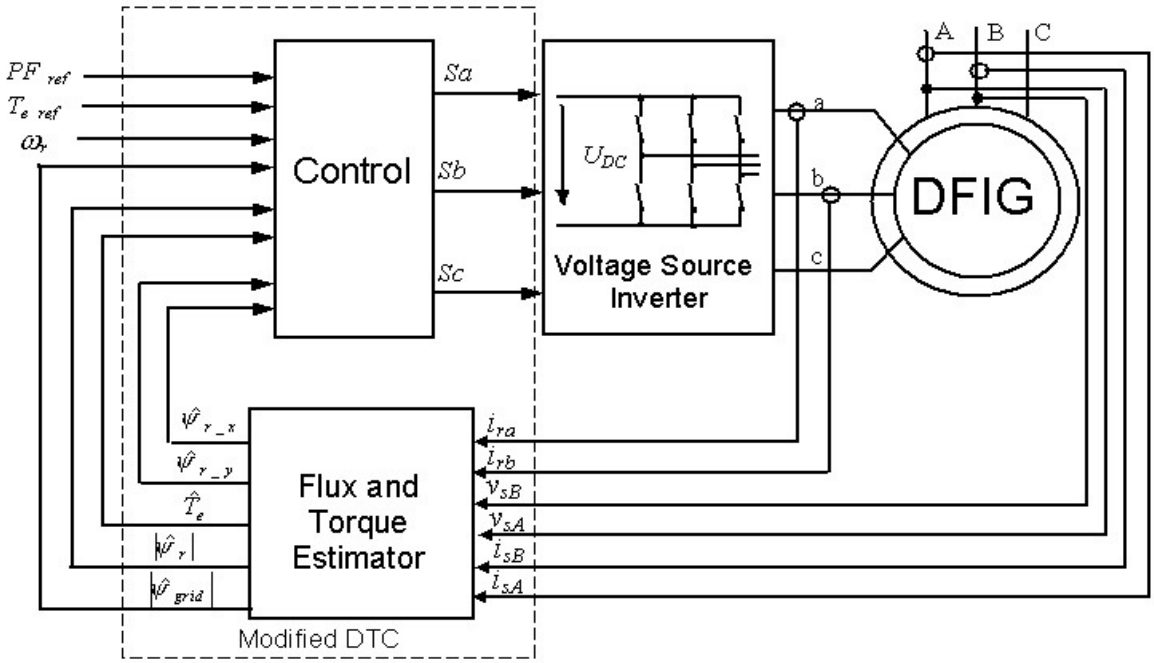

Figure 5. The Block structure of the rotor side frequency converter controlled by modified DTC.

IV. ROTOR OVER-CURRENT PROTECTION

The rotor over-current protection, so called passive crowbar, is connected between the rotor of DFIG and rotor side inverter. The crowbar eliminates high rotor currents during power systems disturbances when the stator of the generator can't be disconnected from the network and generator supports the network. The high currents are induced to the rotor from the stator side when stator-voltage sag due to the short circuit in the network is introduced.

The crowbar circuit that was used in simulations consists of a diode bridge that rectifies the rotor phase currents and a single thyristor in series with a resistor R_{crow} as it is depicted in Figure 6.

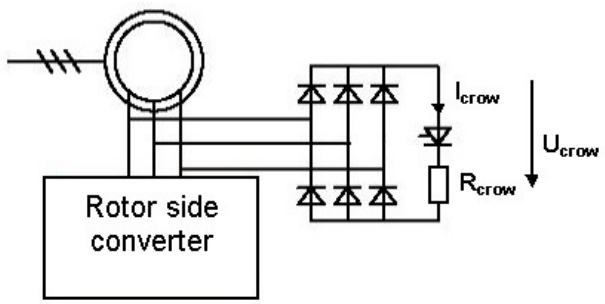

Figure 6. The over-current protection (crowbar) connected between the rotor of DFIG and rotor-side frequency converter.

The thyristor is turned on when the DC link voltage U_{dc} reaches its maximum value. Simultaneously, the rotor circuit is disconnected from the rotor-side frequency converter and connected to the crowbar. The rotor remains connected to the crowbar until the main circuit breaker disconnects the stator from the network.

V. MODEL OF THE NETWORK, TRANSFORMER AND TRANSMISSION LINE

The network is modeled with three-phase voltage source in series with a short circuit inductance and reactance.

The transmission line between the network and the transformer is modeled with its resistance and inductance.

The transformer is represented by simple linear model, i.e. magnetic saturation was not taken into account. The transformer model contains a short circuit resistance and inductance and stray capacitance of the winding.

VI. SIMULATION RESULTS

The simulation analysis was carried out in Matlab – Simulink. The control part, frequency converter, network, transformer and crowbar were modeled in Simulink whereas DFIG was modeled by FEM. The system simulator was running with the time step $T_{step} = 0.5 \cdot 10^{-7}$ s and Forward Euler method has been used. The FEM model of DFIG was running with the time step $T_{stepFEM} = 0.5 \cdot 10^{-4}$ s.

The operation of the 1.7 MVA DFIG before and during the fault in the network was investigated by applying a constant torque T_{ref} = -0.9 p.u. at constant speed 1.1733 p.u. that represents a normal operational condition of wind-power DFIG. The equation of the movement was not included in the model.

The network disturbance has been introduced at time 5.002 s. A symmetrical network 3-phase short circuit has been represented by the stator voltage dip when voltage drops down to 35% of the nominal value. Due to the transient current in rotor of DFIG, the DC-link voltage rises up and the crowbar thyristor is triggered by DC-link over-voltage protection. At the time instance 5.3 s, the generator is disconnected from the network by opening the main circuit breaker.

The simulation results are presented in per-unit system with the base values corresponding to the amplitudes of the respective quantities V_{base} = 563 V, I_{base} = 2.03 kA, T_{base} = 10.9 kNm. The turn's ratio from rotor to stator is t_r = 3.6.

Figure 7 depicts the detailed stator, rotor and DC-link voltages during the network fault.

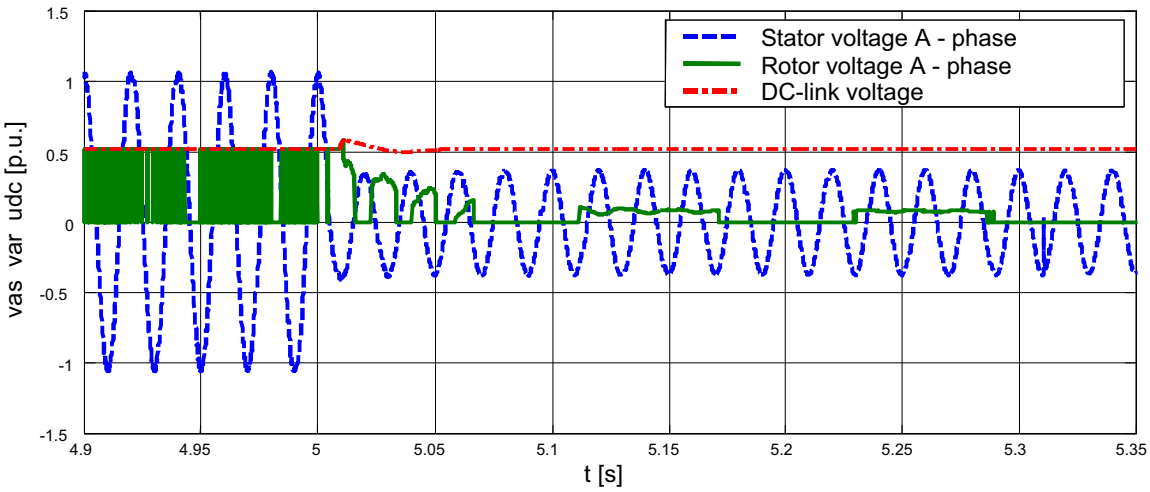

Figure 7. Stator voltage (dash), rotor voltage (solid) and DC-link voltage (dash dot) during network disturbance.

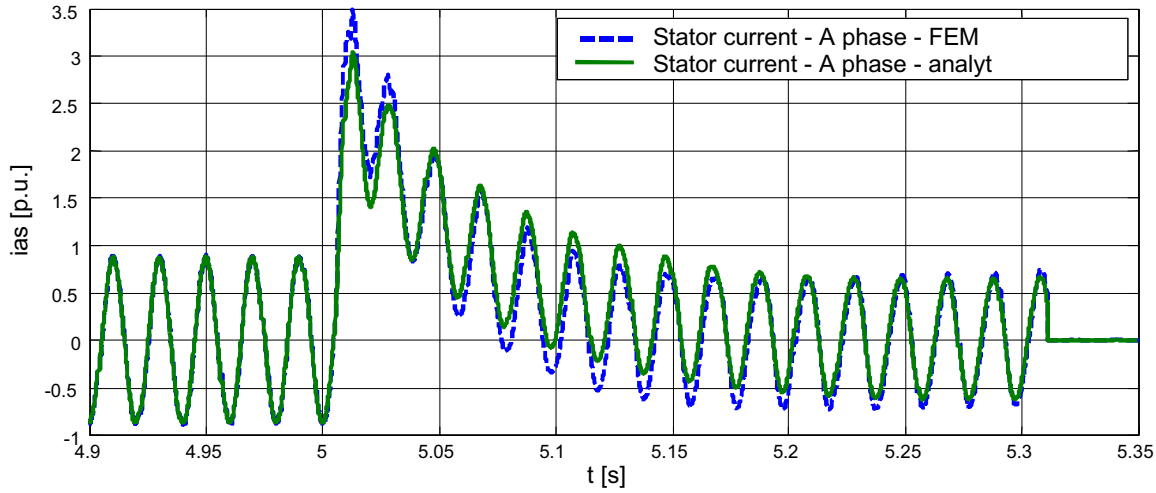

Figure 8. Comparison of the transient stator current obtained from FEM model of DFIG (dash) and from analytical model (solid).

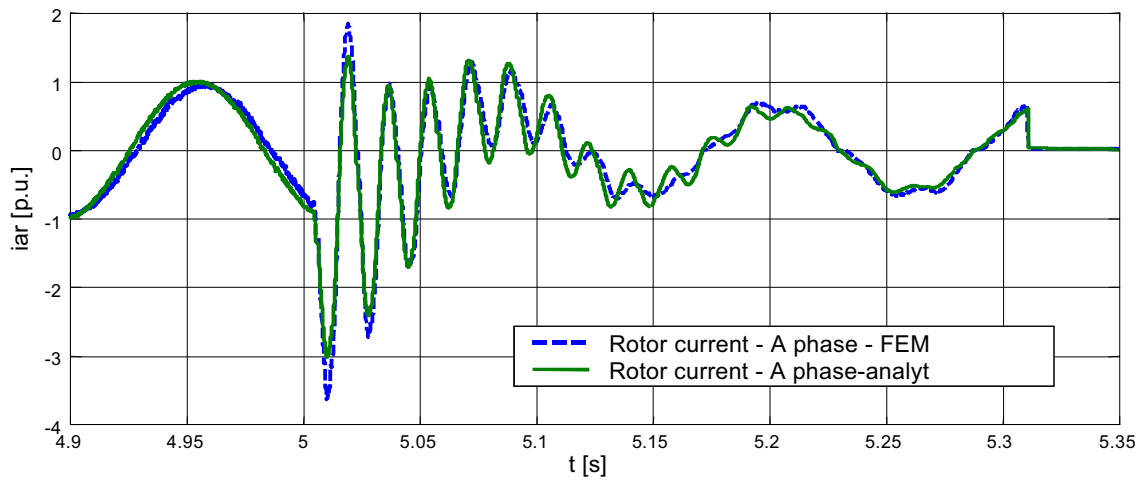

Figure 9. Comparison of the transient rotor current obtained from FEM model of DFIG (dash) and from analytical model (solid).

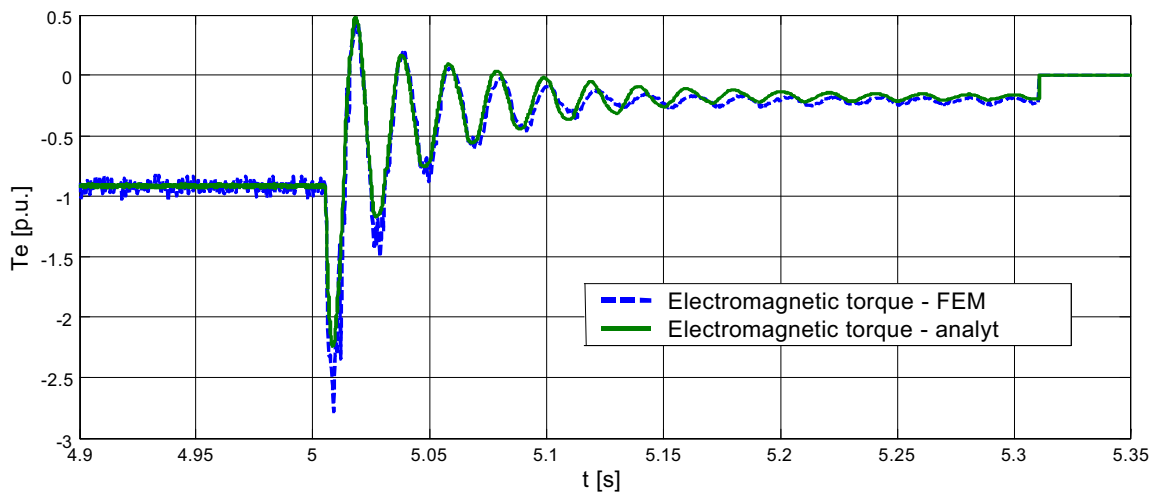

Figure 10. Comparison of the transient electromagnetic torque from FEM model of DFIG (dash) and from analytical model (solid).

Figures 8 and 9 show comparison of the transient stator and rotor current respectively obtained from FEM model of DFIG and from analytical model.

The time variation of the transient electromagnetic torque obtained by means of FEM model that is compared with the transient electromagnetic torque calculated by analytical model is depicted in Figure 10.

VII. DISCUSSION OF THE RESULTS

Figure 7 shows the stator, rotor and DC-link voltage when the network fault is introduced. The network fault causes that amplitude of the stator voltage to drop down to 35% of the nominal value. The high transient currents in the stator and rotor will cause an increase of the DC-link voltage that reaches a maximum value and the control disconnects the rotor from the frequency converter and connects the crowbar to the rotor circuit. After disconnection from frequency converter and connection to the passive crowbar, the DC-link voltage decreases slowly, and after slow transition caused by the control, reaches the nominal value. Shape of the rotor voltage is changed from pulse-modulated waveform to rectified waveform when the crowbar starts to conduct.

The stator transient currents obtained from FEM and analytical model with constant lumped parameters depicted in Figure 8 show the difference of 0.5 p.u. that is about 1 kA at the beginning of the transient. The difference is smaller between 5.05 - 5.2 s. After the generator reaches a new steady state, the simulated stator currents obtained by FEM model and by analytical model show perfect agreement

A Similar situation occurs when comparing the transient rotor currents depicted in Figure 9. During the first peak of the rotor current, the difference between FEM and analytical model is almost 0.6 p.u., that is around 0.5 kA. The difference between the simulated rotor currents obtained from two different models decreases when the DFIG reaches a new steady state.

Figure 10 compares electromagnetic torques calculated by FEM and by means of simple analytical model with constant lumped parameters. The agreement between simulation results is very good except for the beginning of the transient when the difference is around 0.5 p.u. between FEM and analytical model.

All the comparisons of the simulation results show that especially in the beginning of the transient the amplitude of the transient current and torque calculated by FEM model is higher than in case of the simple analytical model with constant lumped parameters. This is mainly due to effect of saturation in stator and rotor leakage inductance that is taken in to account in FEM model.

VIII. CONCLUSIONS

The transient behavior of a doubly fed wind-power induction generator connected to the network and controlled by modified direct torque control during power system disturbances has been studied. The coupled field-circuit model has been used in simulation. The transient currents and electromagnetic torque obtained from FEM model of wind-power doubly fed induction generator were compared with the simulation results obtained by means of "T" equivalent circuit based analytical model with constant lumped parameters. The comparison shows that the transient stator and rotor currents as well as electromagnetic torque have higher peak values in the beginning of the transient in comparison with the analytical model. This is mainly due to effect of the stator and rotor leakage inductances saturation that is taken into account in FEM. The developed simulator is a useful tool in of wind-power doubly fed induction generators and power electronics used for control of the generator as well as for transient simulation studies.

Acknowledgement

The National Technology Agency of Finland, ABB Oy and Fortum Oyj supported this work. Slavomir Seman thanks to Tekniikan edistämissäätiö and Fortum Foundation for financial support.

REFERENCES

[1] E.ON Netz, *Ergänzende Netzanschlussregeln fur Windenergieanlagen*, Dec. 2001, Germany

[2] Ekanayake J. B., Holdsworth L., Wu X. G., Jenkins N., "Dynamic Modeling of Doubly Fed Induction Generator Wind Turbines," *IEEE Transaction on Power Systems,* Vol. 18. No. 2, May 2003, pp. 803 – 809.

[3] Slootweg J. G., Polinder H., Kling W. L, "Dynamic Modeling of a Wind Turbine with Doubly Fed Induction Generator " *Proc. of 2001 IEEE Power Engineering Society Summer Meeting*, Vol. 1, pp. 644 – 649.

[4] Holdsworth L., Wu X. G.; Ekanayake J. B., Jenkins N.: "Comparison of fixed speed and doubly-fed induction wind turbines during power system disturbances" *IEE Proceedings - Generation, Transmission and Distribution*, Volume: 150, Issue: 3, 13 May 2003, pp. 343 – 352.

[5] Tapia A., Tapia G., Ostolaza J.X.,. Saenz J. R: "Modeling and control of a wind turbine driven doubly fed induction generator" *IEEE Transactions on Energy Conversion,* Volume: 18, Issue: 2, June 2003, pp. 194 – 204.

[6] Koessler R., Pillutla S, Trinh L., Dickmander D., "Integration of large wind farms into utility grids (Part 1 - Modeling of DFIG)", *Proc. of 2003 IEEE PES General Meeting.*

[7] Niiranen J., "Voltage Dip Ride Through of Doubly-fed Generator Equipped with Active Crowbar ", *presented at Nordic Wind Power Conference 2004,* 1-2 March 2004, Chalmers University of Technology, Göteborg, Sweden.

[8] Seman S., Niiranen J., Kanerva S., Arkkio A.," Analysis of a 1.7 MVA Doubly Fed Wind-Power Induction Generator During Power Systems Disturbances", *presented at NORPIE 2004,* 14-16 June 2004, Norwegian University of Science and Technology, Trondheim, Norway

[9] Arkkio, A.: *'Analysis of induction motors based on the numerical solution of the magnetic field and circuit equations'*, Doctoral Thesis, Acta Polytech. Scand. Electr. Eng. Ser., No. 59, 1987, Helsinki, Finland, 97 p. http://lib.hut.fi/Diss/198X/isbn951226076X/